Independent Component Analysis for Vision-inspired Classification of Retinal Images with Age-related Macular Degeneration

P. Soliz[1,2], S.R. Russell[2], M.D. Abramoff[2], S. Murillo[3], M. Pattichis[3], and H. Davis[1]
[1]*VisionQuest Biomedical,* [2]*University of Iowa Department of Ophthalmology and Vision Sciences,* [3]*University of New Mexico, Department of Electrical and Computer Engineering*
bert@visionquest-bio.com

Abstract

The purpose of this paper is to present a novel approach for extracting image-based features for classifying age-related macular degeneration (AMD) in digital retinal images. 100 retinal images were classified by an ophthalmologist into 12 categories based on the visual characteristics of the disease. Independent Component Analysis (ICA) was used to extract features at different spatial scales to be used as input to a classifier. The classification used a type of regression, partial least squares. In this experiment ICA replicated the ophthalmologist's visual classification by correctly assigning all 12 images from two of the classes.

1. Introduction

Age-related macular degeneration is the most common cause of visual loss in the United States and is a growing public health problem. Currently, almost 11 million, or 7.6% of all Americans are estimated to have AMD, and it is the cause of blindness for 54% of all legally blind Americans. AMD is a major societal problem in terms of disability and health care costs. For example, severe AMD reduces the likelihood of employment by 61% and salary by 39%, while mild AMD reduces these by 44% and 32% respectively. The estimated annual cost burden from AMD in the U.S. is $30 billion (USD) or about 0.3% of gross domestic product [1]. The prevalence of AMD is expected to double over the next 25 years (CDC).

AMD encompasses diverse and complex fundus appearance changes over the retinal surface and over time. The clinical hallmark of AMD is the drusen deposit, although deposition of other clinically invisible accumulations such as basal laminar and basal linear deposits may be more specific [2]. Drusen appear as white, round or confluent deposits between the basement membrane of the retina pigment epithelium (RPE) and the elastic portion of Bruch membrane [3]. Cross-sectional, longitudinal, and interventional studies by Bressler and others evaluating the role of drusen and other factors have shown that AMD visual outcome or prognosis are related to clinically visible characteristics [4]. These include the presence of large drusen (>125 μm), the presence of multiple intermediate drusen (>63 to <125 μm), the presence of pigmentary abnormalities, "hyperpigmentation", and the contralateral disease severity. The disorder shares with other forms of macular degenerations RPE atrophy and an increased incidence of choroidal neovascularization.

2. Background and Related Work

In order to search for the possible scale-based features that characterize AMD sub-classes, one may wish to use the computer-based analytical techniques of others. Peli and Lahav suggested that computer-based systems could emulate the human in detecting and segmenting features, such as drusen. Uneven illumination artifacts of the retina forced the application of sophisticated adaptive thesholding utilizing Otsu's method, e.g. Morgan et al. and others [5].

Interactive techniques have been applied, driven by limitations of automated segmentation and algorithms. Shin and others since then have reported on interactive systems to quantitate macular drusen [6].These groups added a series of blurring and de-noising convolution filters to remove uneven lighting artifacts. This method was not objective or unbiased. It required a trained grader to optimize the gray level threshold based on their visual interpretation of the drusen margins. Mathematical morphology was further refined by Rapantzikos [7] and Wilson [8].

An alternative approach is one based somewhat on the human vision system. Independent component analysis (ICA) does not explicitly attempt to segment the image into regions representing some type of feature such as drusen. Rather, ICA uses the spatial

information within the context of an image or image set to extract independent components (ICs), or features, that are statistically independent. It may be viewed as a means to discover filters that are spatially and statistically independent and that best describe the information content of the image or image set.

In other words, ICA reduces the redundancy in the samples and thus obtains the unique and independent 'features' that represent the fundus image. There is extensive literature on the use of the ICA methodology for the purpose of extracting statistically independent components (features) from audio and video signals and clinical electrophysiology [9, 10, 11]. We have previously reported on the application of ICA techniques to isolate the changes produced in the retina due to visual stimulation [9]. Our investigators have used and will also apply ICA to compute statistically independent features that are not dependent upon pre-existing notions of what these features are or may represent [12].

ICA applied to sets of images results in independent components, which are arrays of intensity values, and could also be called basis functions, feature detectors, or receptive fields. Within this grant we will refer to these as 'independent components' (see Figure 1). We elected to apply ICA because of the limitations of conventional feature detection techniques, which require prior knowledge of lesion structure and distribution.

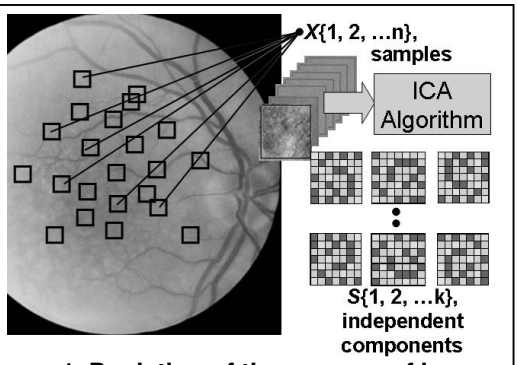

Figure 1. Depiction of the process of image sampling by ICA algorithm, and a subset of the ICs that result. For each color channel, samples X{1,2,3…n}, of scale P pixels by P pixels, are used as arguments for the ICA algorithm. The resulting set of ICs are represented by the P x P grayscale intensity image arrays, S{1,2,3,…,k}.

We and others have worked extensively on mimicking the performance of human graders with considerable success, using algorithms inspired by the physiology of the primate visual cortex [13, 14]. The technique, called pixel feature classification, is based upon characterization of each pixel within the image. A pixel is evaluated on its properties, called 'features', which are its response to less or more complex filters, such as intensity and color, and to highly complex receptive field properties responding to oriented texture patterns. For instance a pixel overlying the center of a retinal hemorrhage is evaluated on the basis of its features and then assigned its probability of belonging to a lesion. Grouping of pixels judged to have high probability of lesion are then assigned a likelihood of being a lesion. Pixel feature classification is powerful, scalable and has been shown to detect certain retinal diseases. The pixel-based approach has been suggested for large-scale diabetic screening and glaucoma progression.

3. Image Processing and Analysis Methods

A set of 100 images centered on the macula were digitized from our database of non-exudative (NE) AMD patients, Age-Related Eye Disease Study (AREDS) simplified scale, category 2 and 3. Image diameters were 2400 pixels or 4.5 micrometers per pixel with 36-bit color depth. Slide images were taken with a 30-degree Zeiss FF4 fundus camera using Ektachome 100.

To perform this demonstration, the ophthalmologist (SRR), categorized the images into 12 phenotypes, two of which were "small distributed drusen, N=8" and "temporally concentrated drusen, N=16." An example of each phenotype is presented in Figure 2a and Figure 2b. Following the AREDS concept of assessing specified regions of interest (ROIs), for example the AREDS grid, two 512 x 512 regions were extracted from the each image. One was centered on the fovea while the second region was of the "outer temporal." The phenotypes to be classified using ICA derived features were: a) small distributed drusen and b) temporally concentrated drusen (see Figure 2).

To test the ICA methodology, five images from the small distributed drusen and six images from the temporally concentrated drusen phenotypes were selected. ICs were collected on each of the two ROIs for each of the images in the two phenotype classes. The ICs were calculated from 2500 samples from each ROI at three different scales, 6x6, 12x12, and 18x18 pixels. Figure 3 illustrates the nature of the ICs (features). This resulted in 3 sets (one for each scale) of 32 ICs each. At this stage it was uncertain which scale

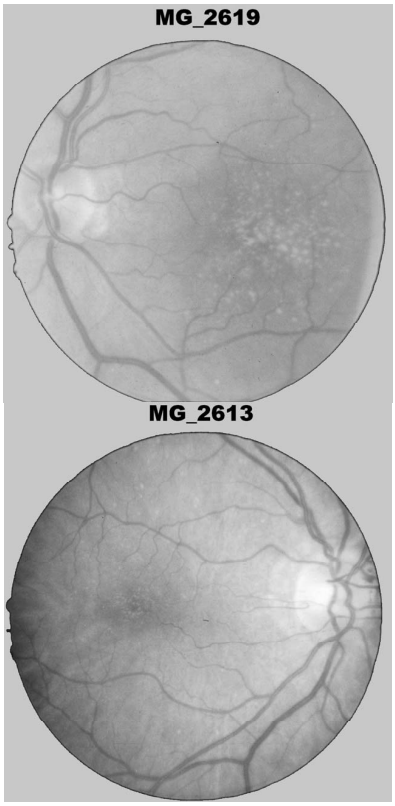

Figure 2. a. Phenotype A is "temporally concentrated drusen." b. Phenotype B is "small distributed drusen." These phenotypes were assigned by the SRR and independently analyzed.

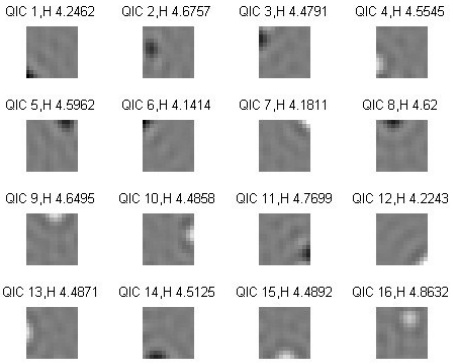

Figure 3 – Central and Temporal ICAs of Image 2619 (Temporally Concentrated Drusen).

of ICA would optimize the differentiating features for the two phenotypes.

Our hypothesis prior to conducting this ICA experiment was that those images classified as the "small temporal drusen" phenotype would display different feature characteristics than the "temporal concentrated drusen" phenotype when comparing features in the central region of interest. Conversely, the "temporal concentrated drusen" phenotype would have features that were distinctly different in the outer temporal region than the "small distributed drusen" phenotype.

Partial least squares (PLS), a form of linear regression, was applied to the set of ICs in order to classify the four types of ROIs. One set of ROIs was for the small distributed drusen, central region (CC) and one set for the outer temporal (OT) [15]. The same two ROIs were used to collect samples for the temporally concentrated drusen phenotype.

4. Results

Figure 4 presents the results of the PLS as applied to the four sets of ICs. This analysis used the 12 x 12 sample sizes. Note that the PLS found clear separation between the features in the four regions. Of particular note is that the features in the central regions for the two classes, small temporal drusen in the central region (smCC) and temporal concentrated drusen in the central region (tempCC) are well separated, as are the features represented by the ICs for the smOT and tempOT.

Figure 5 uses a 6 x 6 sample size, which results in an encoding of a different feature scale by the ICA. Classification results remain unambiguous. Though at this small scale, the features between the two respective regions of the same phenotypes are indistinguishable. That is, small scale features in the central region and temporal region are very similar within a phenotype (see smCC versus smOT in Figure 5).

5. Conclusions

This study has shown that application of ICA can robustly detect and characterize features in fundus images that correspond to the phenotypes visually classified by the observer. In this example we have not determined whether the small central or predominantly temporal drusen phenotypes are enriched for any genetic or environmental factor, although one may be present. The expert observer, SRR, defined the two sets of phenotypes based on his characterization of each fundus based on such visual features as size, distribution, location, concentration, etc. Without the need to develop an algorithm to explicitly mimic the expert observer, ICA extracts implicitly the mathematical features from each image to define the phenotype.

This forms the basis for applying ICA and other computational features to the larger number of images and a broader set of phenotypes.

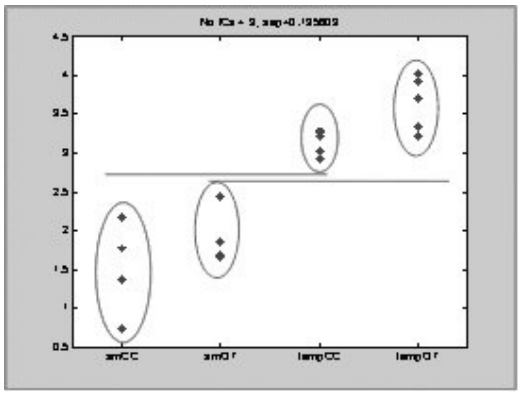

Figure 5 – Same as Figure 6, except for a scale size of 6x6.

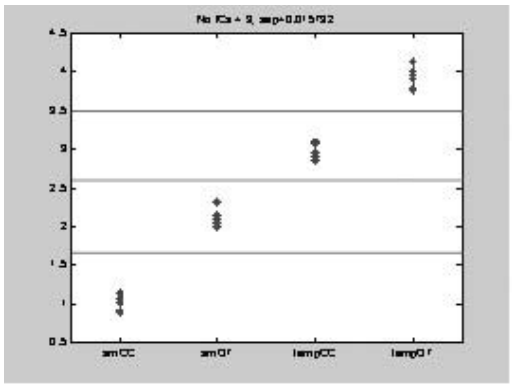

Figure 4 – The results of applying the partial least squares to the set of ICs produced from sampling each of the two ROIs (OT and CC) from the two phenotypes. Scale was 12x12 pixels. Class separation is evident for the two phenotypes: sm = small distributed drusen, and temp = temporally concentrated

10. References

[1] Brown MM. Age-related macular degeneration: economic burden and value-based medicine analysis. Brown GC, Stein JD, Roth Z, Campanella J, and Beauchamp GR. Can J Ophthalmol 40, 277-287. 2005.

[2] Curcio CA, Millican CL. Basal linear deposit and large drusen are specific for early age-related maculopathy. Arch Ophthalmol 1999;117:329-39.

[3] Hageman GS, Luthert PJ, Chong NHV, Johnson LV, Anderson DH, Mullins RF. An integrated hypothesis that considers drusen as biomarkers of immune-mediated processes at the RPE-Bruch's membrane interface in aging and age-related macular degeneration. Prog Retin Eye Res 2001;20(6):705-32.

[4] Bressler SB, Maguire MG, Bressler NM, Fine SL, Group tMPS. Relationship of drusen and abnormalities of the retinal pigment epithelium to the prognosis of neovascular macular degeneration. Arch Ophthalmol 1990;108:1442-7.

[5] Morgan WH, Cooper RL, Constable IJ, Eikelboom RH. Automated extraction and quantification of macular drusen from fundal photographs. Aust.N.Z.J Ophthalmol 22(1):7-12.

[6] Shin DS, Javornik NB, Berger JW. Computer-assisted, interactive fundus image processing for macular drusen quantitation. Ophthalmology 1999;106:1119-25.

[7] Rapantzikos K, Zwervakis M, Balas K. Detection and segmentation of drusen deposit on human retina: potential in the diagnosis of age-related macular degeneration. Med Image Anal 2003;7:95-108.

[8] Wilson M, Yang S, Mitra S, Raman B, Nemeth S, Soliz P. Full automation of morphological segmentation of retinal images - a comparison with human-based analysis. SPIE International Symposium on Medical Imaging 2003.

[9] Barriga ES, Pattichis MP, Ts'o DY, Abramoff M, Kardon R, Kwon Y, Soliz P. Spatiotemporal independent component analysis for the detection of functional responses in cat retinal images. IEEE Transactions on Medical Imaging 2007;26:1035-45.

[10] Calhoun VD, Adali T. Unmixing fMRI with independent component analysis. Engineering in Medicine and Biology Magazine, IEEE 2006;25(2):79-90.

[11] Viergever MA, Maintz JBA, Stokking R, VanDenElsen PA, Zuiderveld KJ. Matching and Integrated Display of Brain Images from Multiple Modalities. In Medical Imaging. Bellingham: SPIE; 1995. p. 2-13.

[12] Barriga ES, T'so D, Pattichis M, Kwon Y, Kardon R, Abramoff M, Soliz P. Detection of low amplitude, in-vivo intrinsic signals from an optical imager of retinal function. Ophthalmic Technologies XVI, Proceedings of the SPIE 2006;6138:66-77.

[13] Abràmoff MD, Alward WL, Greenlee EC, Shuba LM, Kim CY, Fingert JH, Kwon YH. Automated segmentation of the optic nerve head from stereo color photographs using physiologically plausible feature detectors. IOVS 2007.

[14] Niemeijer M, vanGinneken B, Staal J, Suttorp-Schulten MS, Abramoff MD. Automatic detection of red lesions in digital color fundus photographs. IEEE Trans Med.Imaging 2005 May;24(5):584-92.

[15] Wold H. Nonlinear iterative partial least squares (NIPALS) modeling: some current developments. In: Krishnaiah PR, editor. Multivariate Analysis. New York: Academic Press; 1973.